

Using climate to relate water-discharge and area in modern and ancient catchments

Christian Haug Eide*¹, Reidar Müller² and William Helland-Hansen¹

¹Department of Earth Science, University of Bergen, Norway

²Department of Geosciences, University of Oslo, Norway

*Correspondence: christian.eide@uib.no

Running head: Relating water-discharge and catchment area

Submitted to: *Sedimentology*, revision 2, September 22nd, 2017

Number of figures: 5

Number of tables: 3

Number of references: 52

Number of words: 5721 (4244 excluding references)

Supplementary material: A1, Cross-plots and regression lines used to determine values for k and m by runoff class; A2, Spreadsheet containing the database used for calculations and plots.

Abstract

Models relating sediment supply to catchment properties are important in order to use the geological record to deduce landscape evolution and interplay between tectonics and climate. Water-discharge (Q_w) is an important factor in the widely used BQART-model, which relates sediment load to a set of measureable catchment parameters. Although many of the factors in this equation may be independently estimated with some degree of certainty in ancient systems, water-discharge (Q_w) certainly cannot. An analysis of a world database of modern catchments with 1255 relevant entries shows that the commonly applied equation relating catchment area (A) to water-discharge ($Q_w=0.075A^{0.8}$), does not predict water-discharge from catchment area well in many cases ($R^2=0.5$ and an error spanning c. 3 orders-of-magnitude). This is because the method does not incorporate the effect of arid and wet climate on river water-discharge. The inclusion of climate-data into such estimations is an opportunity to refine these estimates, because generalized estimates of palaeoclimate can often be deduced on the basis of sedimentological data such as palaeosol types, mineralogy and palaeohydraulics.

This paper investigates how the relationship between catchment area and river discharge vary with four runoff categories (arid, semiarid, humid, and wet) which are recognizable in the geological record,

33 and modifies the coefficient and exponent of the abovementioned equation according to these classes.
34 Our modified model yields improved results in relating discharge to catchment area ($R^2=0.95$ and error
35 spanning 1 order-of-magnitude) when core-, outcrop- or regional palaeoclimate reconstruction data
36 are available in non-arid systems. Arid systems have an inherently variable water-discharge, and
37 catchment area is less important as a control due to downstream losses. The model here is sufficient
38 for many geological applications and makes it possible to include variations in catchment humidity in
39 mass-flux estimates in ancient settings.

40 **1. Introduction**

41 The extent and quality of geomorphological and subsurface datasets has increased greatly in recent
42 decades, and has made it possible to attempt to reconstruct ancient sedimentary systems from source-
43 to-sink (e.g. Sømme et al., 2009; Galloway et al., 2011; Allen et al., 2013; Michael et al., 2013; Hampson
44 et al., 2014; Holbrook and Wanas, 2014; Bentley et al., 2015). The goals of such studies are to
45 understand the coupling between sediment producing catchments (or *source* areas), sediment-storing
46 sedimentary basins (or *sinks*), the sediment routing systems connecting these systems, and how these
47 interact to record earth history (e.g. Hinderer, 2012; Helland-Hansen et al., 2016). Such studies may
48 be undertaken in order to predict or estimate parameters of sedimentary transport-networks which
49 are inaccessible to study due to erosion or burial (Martinsen et al., 2010), understand the propagation
50 and fidelity of environmental signals through time (Paola et al., 1992; Romans et al., 2016), and
51 characterise the evolution of past landscapes (e.g. Sømme et al., 2009; Bhattacharya et al., 2016; Eide
52 et al., *in press*).

53 The BQART-approach, based on an empirical model relating sediment load in modern rivers to
54 catchment parameters, was developed by Syvitski and Milliman (2007). This method has recently been
55 applied to investigate ancient deposits (Weight et al., 2011, Sømme et al., 2013, Allen et al., 2013). The
56 details are outlined below, but the model is on the form of an equation with the following parameters
57 valid for ancient systems: sediment load, catchment area, catchment relief, catchment lithology,
58 catchment temperature, degree of glacial cover, and water-discharge of the river. Depending on the
59 available dataset and the questions asked, some of these parameters may be measured, estimated or
60 modelled, while some parameters are kept as variables (e.g. Sømme et al., 2013; Allen et al., 2013;
61 Eide et al., *in press*).

62 In the absence of good palaeohydraulic data, such as dimensions of trunk channels and bedforms
63 within them (e.g. Bhattacharya and Tye 2004; Holbrook and Wanas, 2014), or extremely well-
64 constrained modern analogues with well-chosen regional curves (Davidson and North, 2009), water
65 discharge in ancient rivers is difficult to estimate well. In most studies using the BQART-approach in
66 ancient systems, water-discharge is estimated using a power-law function relating river discharge (Q_w)
67 and catchment area (A), which was proposed by Syvitski and Milliman 2007:

$$68 \quad \text{Eq. 1: } Q_w = kA^m$$

69 where Q_w is water-discharge in m^3/s , A is catchment area in km^2 , k is an empirical constant set to 0.075,
70 and m is an empirical constant set to 0.8. However, some catchments are much drier than others (e.g.
71 Fig 1; Beck et al., 2015), and this is not taken into account in this model. Therefore, using this model
72 may lead to large, systematic errors in the estimation of water-discharge (up to 2.5 orders of
73 magnitude, excluding outliers, c.f. Figs. 2A, 3).

74 Because generalized interpretations of large-scale climate can be made from simple geological
75 observations (e.g. Retallack, 1997; Parrish, 1998; Hay, 2008), it should be possible to improve estimates
76 of water-discharge of ancient catchments if geological data are available. In this paper, a global
77 database of catchment properties of rivers discharging into the ocean (Milliman and Farnsworth, 2011)
78 is used to improve the model for water-discharge from catchments. This model is presented as Eq. 1.
79 It is shown that discharge may be predicted from catchment area (and *vice versa*) at an acceptable
80 level of precision and accuracy by using *the method presented in this paper*: choosing appropriate
81 values for k and m in Eq. 1 by classifying studied deposits into four runoff classes (arid, semiarid, humid
82 and wet). These classes can readily be estimated by geological palaeoclimatological indicators (e.g.
83 palaeosol types, presence of climate-sensitive sedimentary environments such as evaporites and
84 aeolian dunes) and published palaeogeographic reconstructions. This yields simple, reliable and well-
85 constrained inputs to source-to-sink models.

86 Thus, the goals of this paper are threefold: (1) to present an improved model for estimating
87 relationship between river discharge and catchment area for different climate types in modern
88 environments, (2) to outline how these relationships may be employed in deep time stratigraphic
89 successions where proxies for palaeoclimate can be retrieved, and (3) to investigate in which settings
90 this model might be inappropriate.

91 2. Background

92 2.1 The BQART-model

93 In deep-time systems ($\gg 1$ Ma), significant parts of sediment sinks are often preserved in
94 sedimentary basins, but the sediment source areas are commonly eroded or extensively modified
95 (e.g. Blum and Pecha, 2014; Eide et al., 2016; Eide et al., *in press*). Ancient catchment areas may be
96 reconstructed to some degree using different thermochronological methods, such as detrital zircon
97 and fission track data (e.g. Gallagher et al., 1998; Fedo et al., 2003; Lisker et al., 2009). However,
98 these methods require significant skill, time, funds and material. Thus, a popular and well-established
99 method used to investigate source-to-sink relationships in ancient systems is to apply the BQART-
100 method developed by Syvitski and Milliman (2007) (e.g. Weight et al., 2011; Allen et al., 2013;
101 Sømme et al., 2013). It is an empirical model, based on global regression of modern catchment data,
102 and uses the following equation for catchments with average mean temperatures $> 2^\circ\text{C}$:

$$103 \quad \text{Eq. 2: } Q_s = \omega B Q_w^{0.31} A^{0.5} R T$$

104 where Q_s is sediment load (Mt/yr), ω is a constant of proportionality set to 0.0006, Q_w is long term
105 water-discharge (km^3/yr), A is catchment area (km^2), R is maximum relief in the catchment (km), T is
106 long-term average temperature in the catchment ($^\circ\text{C}$) and B is a factor based on the glacial erosion
107 factor (I), lithology (L), trapping efficiency of lakes and reservoirs (T_e), and human-influenced soil
108 erosion (E_h), given by the following equation:

$$109 \quad \text{Eq. 3: } B = IL(I-T_e)E_h$$

110 In non-glaciated, pre-human catchments, the factor B simplifies to lithology (L) only. Some inherent
111 limitations to this model should be pointed out: it only includes suspended load (which is commonly
112 taken to be $> 90\%$ of total load); and that it is based on time series in the order of 30 years, and thus

113 underestimates sediment transport related to rare, catastrophic events (Milliman and Farnsworth,
114 2011). Furthermore, although water-discharge is a weak variable in the Eq. 2 (i.e. it has the lowest
115 exponent), it is also the most *variable* of the variables. For natural systems in the database (Milliman
116 and Farnsworth, 2011), water-discharge varies across six orders-of-magnitude, versus 5 orders-of-
117 magnitude for area, three orders-of-magnitude for relief, two for temperature and one for lithology.
118 Thus, compared to the natural variability of the other factors, it the second-most important variable
119 controlling sediment discharge.

120 **2.2. Catchment relief, lithology and temperature**

121 For ancient catchments, factors such as relief, bedrock type, catchment palaeotemperature and
122 presence and extent of glaciers may often be approximated based on regional geological evidence,
123 and from published global data. Relief (R) may be estimated through modern topographic analogues
124 (systems draining uplifted rift shoulders, flat plains or large orogens; c.f. Parrish, 1998), fission track
125 analysis, or preserved palaeosurfaces (e.g. Leturmy et al., 2003; Sømme et al., 2009). Bedrock type (L)
126 may be estimated through provenance studies of detrital mineralogy and clast composition, and
127 extrapolation of geological maps into now eroded areas. Catchment temperature (T) may be estimated
128 from global palaeo-general circulation models (e.g. Sellwood and Valdes, 2006), isotope-based
129 palaeotemperature-estimates (Sun et al., 2012), reconstructions based on plant communities and
130 palynofloras (e.g. Paterson et al., 2016), and geological evidence such as palaeosol types (e.g. Wright,
131 1990; Mack and James, 1994; Kraus, 1999; Parrish, 1998; Retallack, 2001; Müller et al., 2004; Nystuen
132 et al., 2014).

133 **2.3. Catchment area**

134 Catchment area (A) is in most cases hard to constrain accurately in ancient systems, due to erosional
135 and tectonic modification. In systems with a marked topographic axis, such as in convergent and
136 transpressive regimes, catchment area may be estimated using distance to the topographic axis and
137 Hack's Law (Hack, 1957; Rigon et al., 1996). However, these are also the most short lived and unstable
138 source-to-sink systems, and sediment transport networks are prone to change through time
139 (Woodcock, 2004).

140 **2.4. Water-discharge, climate and runoff**

141 In uplifted, dissected and well-exposed systems, water-discharge (Q_w) may be estimated using
142 palaeohydraulic methods based on exposed trunk river channel dimensions (Bhattacharya and Tye,
143 2004; Holbrook and Wanas, 2014). These methods may also be applied to subsurface datasets:
144 attribute maps derived from 3D-seismic data may give full plan view control of parts of deposits of
145 fluvial systems, and thickness of channels and bedforms can be measured in core. However, such
146 comprehensive datasets are commonly not available. In cases where very well-constrained modern
147 analogues have been determined, regional hydraulic geometry curves from comparable modern
148 systems could be applied to derive catchment area and water-discharge (Davidson and North, 2009).
149 However, there is generally significant uncertainty in defining suitable analogues for regional hydraulic
150 geometry curves, especially in ancient times with varying global climates and equator-pole
151 temperature gradients (c.f. Hay, 1998).

152 Syvitski and Milliman (2007) presented Eq. 1 as a simple method to estimate water-discharge from
153 catchment area. However, this method is clearly inadequate to relate discharge and catchment area,
154 because two equally large catchments in different climates will have very different water-discharge

155 (Fig. 1), owing to varying amounts of rainfall and evapotranspiration (e.g. Mu et al., 2007; Beck et al.,
156 2015).

157 The *runoff* (ratio of annual river discharge to catchment area) of rivers varies with climate (Fig. 1).
158 Runoff of rivers is commonly given in $\text{mm km}^{-1}\text{yr}^{-1}$, and is therefore easily compared with catchment-
159 averaged rainfall. The *runoff efficiency* of a catchment is the ratio of runoff to catchment-averaged
160 rainfall, and is commonly lower in drier catchments due to higher evapotranspiration and infiltration
161 losses, and high in wetter catchments due to moister soil (e.g. McCabe and Wolock, 2016). Thus, runoff
162 of rivers is strongly dependent upon climate, as more precipitation will lead to higher runoff due to
163 increase in both the availability of water, and increase in runoff efficiency.

164 **3. Dataset and methods**

165 This study is based on analysis of the global database of catchment properties presented by Milliman
166 and Farnsworth (2011), which collates a wealth of information from modern catchments debouching
167 into the ocean, such as sediment supply, relief, climate, location, and most importantly for this study:
168 catchment area and water-discharge. These systems are investigated using cross plots and power law
169 regression (Figs. 2-4), and are further investigated using published data and publically available
170 satellite imagery. The database (Milliman and Farnsworth, 2011) contains 1531 entries, and 1255 of
171 these have information about catchment area and river discharge. Furthermore, 72 of these systems
172 have information about pre-dam discharge. For these systems, the pre-dam discharge is used to
173 provide values for runoff and discharge. It is worth noting that many of the rivers with pre-dam
174 discharge-values are well-known rivers with extensive water management systems (e.g. Murray-
175 Darling, Nile, Colorado), indicating that these are the catchments which have been changed most by
176 human intervention. Although most other catchments will likely have some amount of damming or
177 watercourse interventions, this cannot be accounted for using the utilized database.

178 The boundaries for runoff categories employed by Milliman and Farnsworth (2011) in their
179 compilation, (arid 0-100; semiarid 100-250; humid 250-750; and wet $>750 \text{ mm km}^{-1}\text{yr}^{-1}$) gave good
180 results and are adopted in this study.

181 **4. Results**

182 **4.1. Analysis of accuracy using fixed constants in Eq. 1**

183 Figure 2A presents the actual catchment area for all catchments in the database, versus predicted
184 catchment area using Eq. 1 and the fixed constants from Syvitski and Milliman (2007). This plot shows
185 that using this method, catchment area is underestimated for arid systems, and overestimated for wet
186 systems. Furthermore, this method leads to large variation in error (c. 2.5 orders of magnitude when
187 outliers are excluded) of estimation of catchment areas for arid systems (Fig. 2A). Semiarid, humid and
188 wet systems generally show little variation in error and generally constrain the input with some
189 accuracy (within 30x).

190 Figure 3 presents the runoff of all systems in the database (Milliman and Farnsworth, 2011), plotted
191 against the error of the catchment area estimation. Using fixed values for k and m in Eq. 1, error in the
192 catchment area estimation is dependent on runoff alone. Using this method, catchment area is
193 systematically and strongly underestimated in arid systems (median error: 0.06x), systematically

194 underestimated in semiarid systems (median error: 0.4x), correctly estimated for humid systems, and
195 systematically overestimated for wet systems (median error: 4x).

196 **4.2. Determination of coefficients in Eq. 1 for each runoff class**

197 In order to obtain new constants for each of the four runoff classes, power-law regression was
198 performed on cross plots of catchment area versus runoff for each of the four runoff classes (Appendix
199 A1). Determined best-fit exponents and correlation coefficients (R^2) are presented in Table 1. Plots of
200 actual versus estimated catchment area using the proposed model are presented in Fig. 4. These show
201 a significant improvement compared to using fixed constants (c.f. Fig. 2A), but also large variations in
202 arid systems. The previous and the proposed model are compared in Figures 2B and 2C, including and
203 excluding arid systems, respectively. This shows that estimates of catchment area are significantly
204 improved using the proposed method. However, catchment area estimation appears to be too variable
205 to be useful in arid catchments.

206 **5. Discussion**

207 **5.1. Recognition of runoff classes in ancient deposits**

208 Defining the runoff class of ancient deposits makes estimations of river discharge and catchment area
209 more accurate (Fig. 2B, Table 1). The key assumption in this work is that the runoff classes defined in
210 this study would correspond to geologically observable factors. As the study of ancient climates is a
211 science in itself, only a superficial overview can be presented here. For a comprehensive view, see
212 important works by e.g. Hay (1998; 2008), Hay and Floegel (2012); Parrish (1998) and Driese et al.
213 (2005).

214 There are several depositional features which are preserved in sedimentary systems (c.f. Fig. 5) and
215 observable in the geological record (Table 2) that makes it possible to interpret whether deposition
216 occurred under arid, semiarid, humid or wet conditions. These include particular palaeosol types
217 (calcretes, oxisols, coals) and features (e.g. Mack and James, 1994; Bestland, 1997), aeolian dunes,
218 plant communities (e.g. Paterson et al., 2016), soil color, mineralogy, fluvial architectures (Retallack,
219 2001; Nystuen et al., 2014), and isotopes (Cerling, 1984). However, care must be taken as climate in
220 the basin can be different from that in the catchment area (Fig. 1; c.f. Nystuen et al., 2014).
221 Furthermore, it must be pointed out that several of the features mentioned here are not controlled by
222 runoff alone, but are also partly a function of temperature and evaporation. Models for estimating
223 runoff in cold and polar systems are not well-developed, and the method presented here would likely
224 not work well in such systems.

225 **5.2. Comparison to method using fixed constants**

226 Comparison between the method presented here (varying constants by climate class) versus the
227 method using fixed constants in Eq. 1 is presented in Fig. 3. This figure shows that the method using
228 fixed constants performed well for systems with runoff within the ranges 200-800 $\text{mm km}^{-1} \text{yr}^{-1}$ (Fig.
229 3), a range which contains 43% of the catchments in the database. For the wet category, which contains
230 30% of the data, the proposed method is significantly better than using fixed constants (Fig. 3).
231 Furthermore, this study shows that it is difficult to estimate runoff for arid systems, as annual discharge
232 is not primarily controlled by catchment size in such systems. Still, the proposed method decreases the
233 error of arid systems by two orders of magnitude. Finally, this study shows that water-discharge and

234 catchment area can be related with a high degree of confidence if the runoff class of the system can
235 be determined, with the exception of arid systems.

236 The results of sediment mass-flux calculations from ancient catchments, made using the BQART-
237 approach (Syvitski and Milliman, 2007), change significantly when runoff class of the studied system is
238 taken into account. The difference for sediment load (Q_s in Eq. 2) calculated using water-discharge from
239 the two methods presented herein (fixed constants versus variable constants for each class) is greatest
240 for small, dry catchments and for large, wet catchments (Table 3). For small (100 km^2) arid and
241 semiarid catchments, using varying constants in Eq. 1 yields a 69% and 40% decrease in sediment load,
242 respectively, compared to results using fixed constants. For large (10^6 km^2 , 'continental' scale
243 catchments) humid and wet catchments, using variable constants for each climate class gives a 36%
244 and 73% increase in sediment load, respectively. Thus, this study shows that it is important for studies
245 using the BQART-approach in ancient systems to take runoff into account, not only catchment
246 temperatures.

247 **5.3. Human influence and validity of methods**

248 The majority of world catchments have some degree of human influence. In the database (Milliman
249 and Farnsworth, 2011), 72 of the 1255 catchments also have data about pre-dam discharge. 29% of
250 these are classified as arid based on runoff, 29% are semiarid, 31% are humid and 11% are wet. Post-
251 dam discharge decrease in 71 of the 72 catchments, and the reduction ranges from 11% (Tapti, India)
252 to 99% (Colorado, USA), and no correlation between the amount of decrease and runoff or catchment
253 area exists. This indicates that post-dam discharge reduction is mainly determined by water
254 management strategies and water demand, not natural properties inherent to catchments, making
255 this difficult to correct for in a global dataset.

256 It is worth noting that the catchments with pre-dam discharge-data in the database often represent
257 highly populated catchments with well-known and large water management projects, such as the Nile
258 (NE Africa), Orange (S Africa), Los Angeles (USA), Colorado (USA) and Huanghe (China) (c.f. Fig. 1). It
259 may therefore be speculated that discharge from catchments without pre-dam discharge data is
260 generally less affected by human intervention than catchments with pre-discharge data. Thus, it is
261 estimated that the coefficients presented here, which are conditioned to post-dam catchment
262 discharge, might underestimate final discharge to some degree. However, further research would be
263 needed to constrain this amount.

264 **5.4. Large discharge variations in arid systems**

265 This study illustrates that discharge from arid catchments is not controlled to a great degree by
266 catchment area. This is not surprising, as rivers in arid catchments show flashy discharge and have
267 significant downstream discharge losses. Because of this, discharge during one flood event may be
268 greater than the discharge of several years combined (e.g. Tooth, 2000; Milliman and Farnsworth,
269 2011). Thus, discharge of rivers in arid catchments is more dependent upon the amount and location
270 of rainfall during one single flood, and the degree and extent of wetting prior to the flood, than the
271 size of the catchment itself. Large arid catchments have the potential to lose significant amounts of
272 water through infiltration and evaporation, and this is particularly likely for parts of the catchment
273 located far from the river mouth. This leads to low predictability of discharge in arid systems for a
274 method which uses catchment area as input.

275 **6. Conclusions**

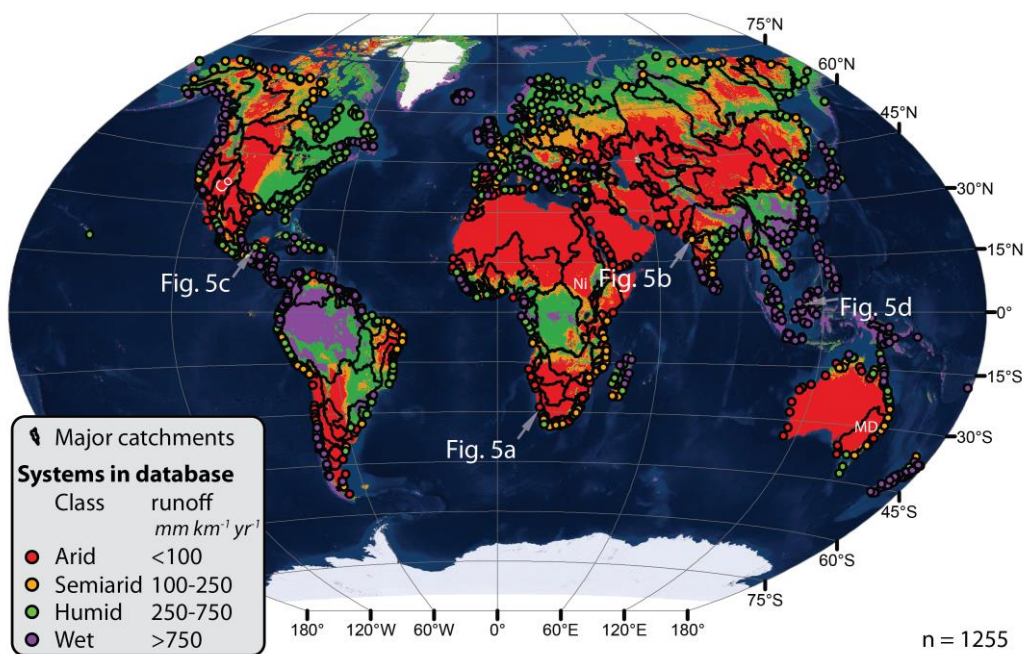
276 When reconstructing ancient source-to-sink systems, estimates of water-discharge (Q_w) and
277 catchment area (A) are crucial in order to apply mass-balance models. Here, it is demonstrated that
278 the previous method ($Q_w=0.075A^{0.8}$) works reasonably well in semiarid and humid settings, but that it
279 yields a significant overestimation of catchment area in wet systems, and a significant underestimation
280 of catchment area in arid systems. Because catchment climate can be readily defined from geological
281 evidence, a new method with different exponent and coefficient for each runoff class is presented.
282 This study shows that it is possible to achieve improved correspondence between measured and
283 predicted values (R^2 -values of 0.95) in non-arid modern systems. However, arid systems show too high
284 variability to be reliably predicted in this way, because of the large temporal variation in rainfall and
285 high downstream losses discharge for arid systems. This has important implications for studies which
286 employ the BQART-method in ancient systems, because climatic changes may strongly influence
287 sediment flux from catchments.

288 **7. Acknowledgements**

289 We acknowledge reviewers John Holbrook and Vernon Manville for useful comments and suggestions which greatly improved this
290 manuscript. This work has been funded by the Trias North project under grant 234152 from the Research Council of Norway and with financial
291 support from Tullow Oil Norge, Lundin Norway, Statoil Petroleum, Edison Norge and Dea Norge. The authors would also like to thank all
292 scientists in general, and J.P.M. Milliman and K.L. Farnsworth in particular, who make full datasets available to the public for the advancement
293 of science.

294 **8. Captions**

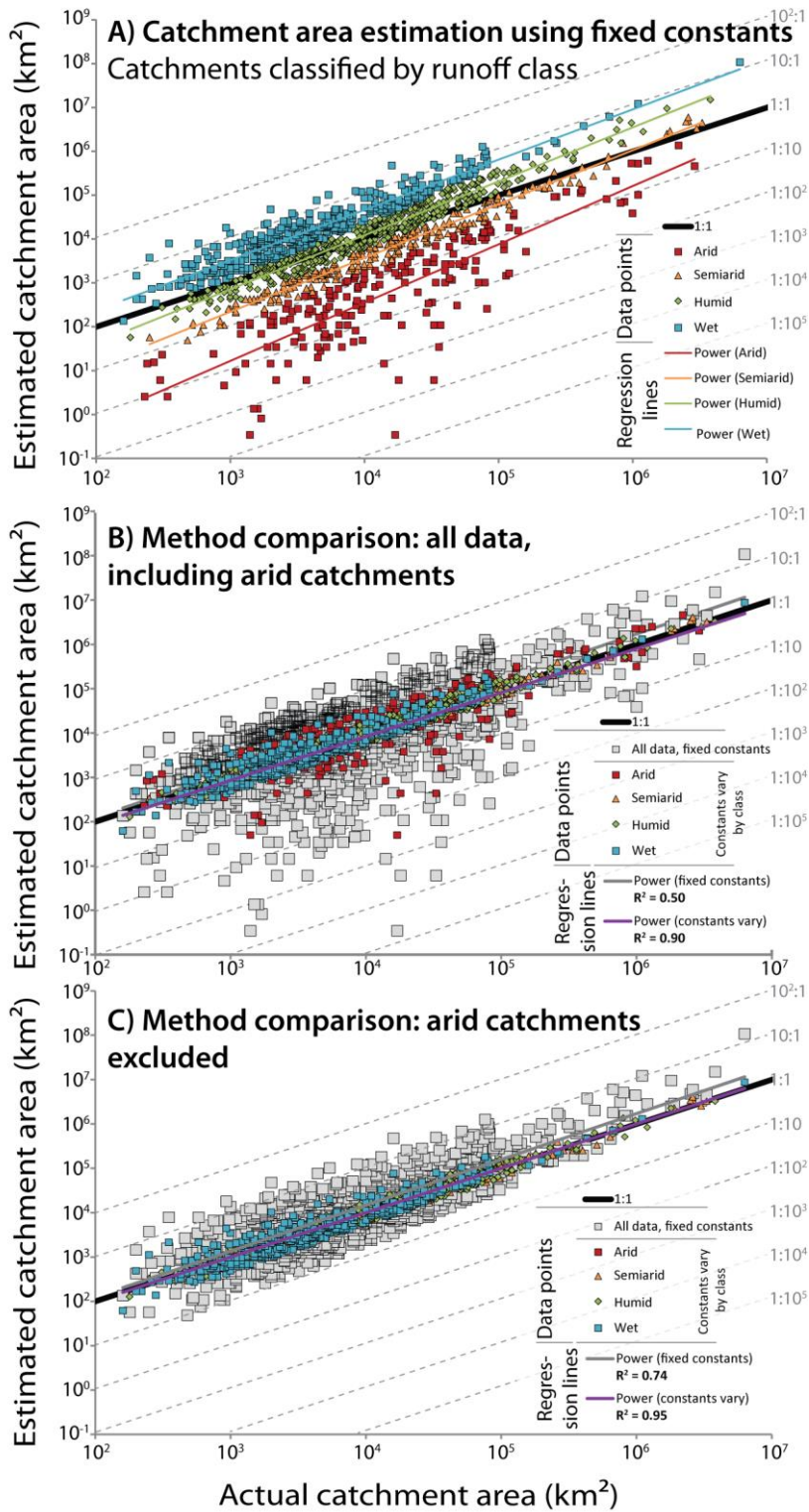
295



296

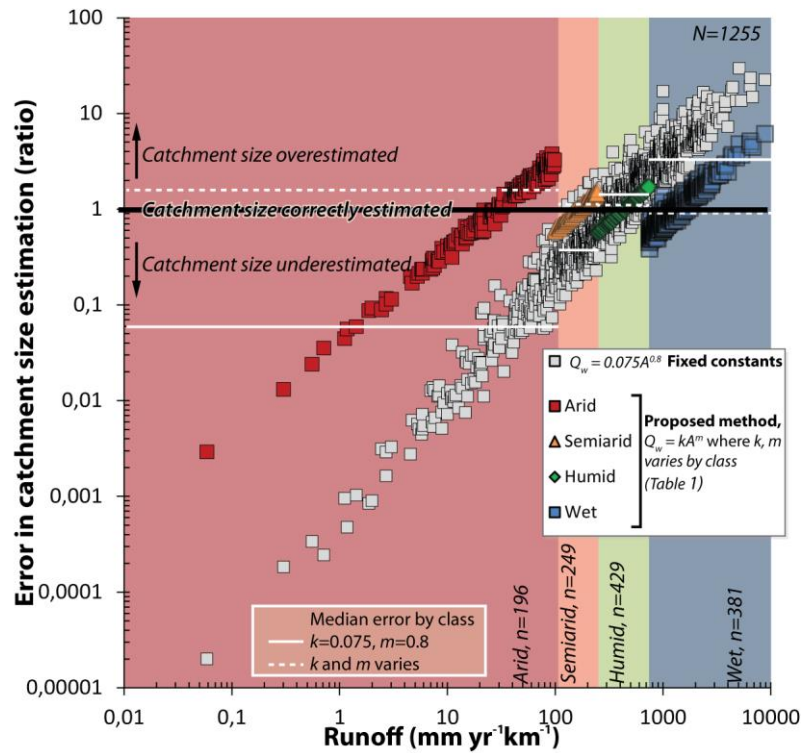
297

298 Fig. 1: World map showing present-day global runoff (Beck et al., 2013; 2015), locations of river outlets from
299 catchments in the database of modern systems (Milliman and Farnsworth, 2011), and major world catchments.



300

301 Fig. 2: Cross plots showing relationship between actual and estimated catchment area using different constants
 302 k and m (Table 1). Data points are from the catchment database of Milliman and Farnsworth (2011), $N=1255$. A)
 303 Cross plot showing estimates of catchment area of modern catchments using fixed values for k and m ($k=0.075$
 304 and $m=0.8$) across different runoff classes. Note the systematic underestimation and large spread of errors in
 305 estimation of arid catchment area, and the systematic overestimation of wet catchment area. B) Comparison of
 306 results using fixed k and m , versus varying k and m based on runoff class, as proposed herein. C) Comparison of
 307 results using fixed k and m , versus varying k and m based on runoff, for all data excluding arid systems (i.e. plot
 308 is as (A) without arid systems).

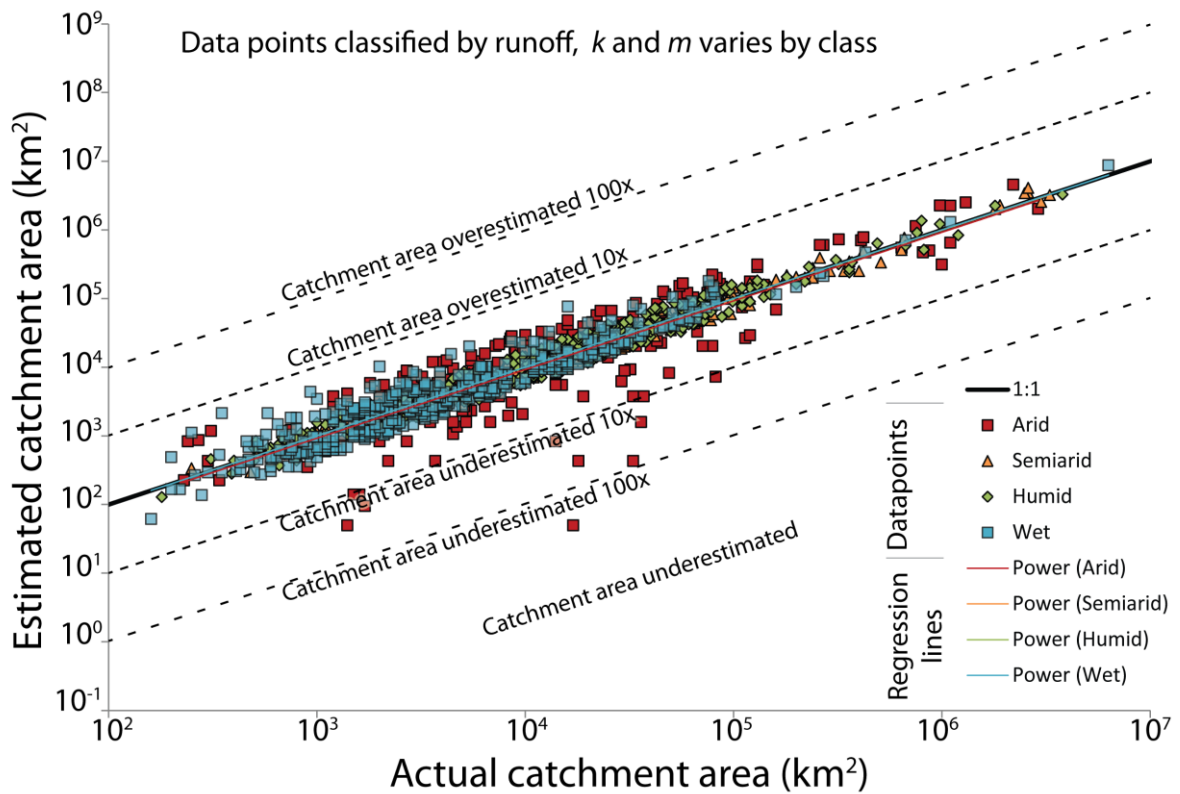


309

310

311 Fig. 3: Runoff and error in catchment area estimation using fixed versus variable constants in Eq. 1 for 1255
 312 modern catchments (from Milliman and Farnsworth, 2011). An error value of 1 indicates no error in the
 313 catchment estimation, and error values of 0.1 and 10 indicate ten times under- and overestimation of catchment
 314 area, respectively. Note the large errors associated with wet and arid systems using fixed constants (grey
 315 squares), and how this improves significantly using the method proposed in this contribution (coloured symbols
 316 for each class).

317



318

319 Fig. 4: Cross plots showing actual catchment area versus catchment area estimated from water-discharge in
 320 modern catchments, using Eq. 1 and different values of constants k and m for each runoff class (Table 1). Note
 321 the improved fit between actual and estimated area compared to Fig. 2A, and note that errors are still large for
 322 arid systems. See Table 1 for correlation coefficients. Data points are from the catchment database of Milliman
 323 and Farnsworth (2011), $N=1255$.

324



325

326 Fig 5: Satellite images of sedimentary systems in the four runoff categories, showing the clearly different
 327 landscapes that would be expressed as detectable geological indicators. For locations, see Fig. 1. A) Orange River,
 328 Namibia. Runoff = $4.5 \text{ mm km}^{-1} \text{ yr}^{-1}$. B) Narmada River, India. Runoff = $230 \text{ mm km}^{-1} \text{ yr}^{-1}$. C) Grijalva River, Mexico.
 329 Runoff = $460 \text{ mm km}^{-1} \text{ yr}^{-1}$. D) Rajang, Indonesia. Runoff = $2150 \text{ mm km}^{-1} \text{ yr}^{-1}$. Image data are © Google 2016.

330

331 **Table 1:** Runoff category limits, constants k and m , and correlation coefficients (R^2) for each of the
 332 populations plotted in Figures 2 and 4.

333 **Table 1:** Runoff category limits, constants k and m , and correlation coefficients (R^2) for each of the
 334 populations plotted in Figure 2.

Model	Class	Runoff (mm yr ⁻¹ km ⁻¹)	k	m	R ²
Eq. 1, fixed constants	All data	>0	0.075	0.8	0.50
	All data, arid excluded	>100	0.075	0.8	0.74
Proposed method: Eq. 1, constants vary by class	Arid	0-100	0.0005	1.0633	0.72
	Semiarid	100-250	0.0063	0.9824	0.98
	Humid	250-750	0.0161	0.9839	0.96
	Wet	>750	0.0873	0.9164	0.99
	All data	>0	varies	varies	0.90
	All data, arid excluded	>100	varies	varies	0.95

335

336

337 **Table 2:** Generalized criteria for determining palaeoclimate from geological indicators.

	Arid	Subarid	Humid	Wet	Notes	References
Runoff (mm km ⁻¹ yr ⁻¹)	<100	100-250	250-750	>750	-	-
Palaeosol types	Calcisols, gypsisols, entisols, inceptisols	Calcisols, vertisols	Argillisols, spodsols, gleysols, histosols	Histosols, gleysols, Oxisols, agrillisols	Extensive well-drained soils not expected in sedimentary basins in wet and humid systems	Mack and James, 1994
Root types	Deep tap-roots	Deep tap-roots	-	Tabular mat		Retallack, 1997; 2001;
Mineralogy	Presence of gypsum, carbonate.	Presence of carbonate	-	High proportion of quartz versus feldspar,	Quartz/feldspar ratio and ratios of smectite and kaolinite to immature clay minerals (illite and chlorite) increase due to increased chemical weathering under higher temperature and humidity.	Robert and Kennet, 1994; Retallack, 1997; Nystuen et al., 2014;
River architectures	Strongly ephemeral/flashy	Ephemeral/flashy	Perennial	Perennial	-	Tooth, 2000; Nystuen et al., 2014
Other:	Nearby aeolian or evaporite deposits	-	-	-	-	-

338

339

340 **Table 3:** Change in calculated sediment load using the proposed method to calculate water discharge
341 as input to the BQART-approach (Eq. 2; Syvitski & Milliman, 2007), compared to using fixed
342 constants, keeping all other variables equal.

343

Area, km ²	Modern river at this scale	Change in calculated sediment load			
		Arid	Semiarid	Humid	Wet
6300000	Amazon	-24 %	12 %	52 %	84 %
1000000	Ganges	-35 %	1 %	36 %	73 %
100000	Colorado	-46 %	-11 %	20 %	59 %
10000	Severn	-55 %	-22 %	5 %	46 %
1000	Dee	-63 %	-31 %	-8 %	34 %
100	-	-69 %	-40 %	-19 %	24 %

344

345

346

347

348 **9. References**

349 Allen, P.A., Armitage, J.J., Carter, A., Duller, R.A., Michael, N.A., Sinclair, H.D., Whitchurch, A.L.,
350 and Whittaker, A.C. (2013). The Qs problem: Sediment volumetric balance of proximal
351 foreland basin systems. *Sedimentology*, 60, 102-130.

352 Beck, H.E., De Roo, A. and van Dijk, A.I. (2015). Global maps of streamflow characteristics
353 based on observations from several thousand catchments. *Journal of Hydrometeorology*, 16,
354 1478-1501.

355 Beck, H.E., Dijk, A.I., Miralles, D.G., Jeu, R.A., McVicar, T.R. and Schellekens, J. (2013). Global
356 patterns in base flow index and recession based on streamflow observations from 3394
357 catchments. *Water Resources Research*, 49, 7843-7863.

358 Bentley, S.J., Blum, M.D., Maloney, J., Pond, L., and Paulsell, R. (2015). The Mississippi River
359 source-to-sink system: Perspectives on tectonic, climatic, and anthropogenic influences,
360 Miocene to Anthropocene. *Earth-Science Reviews*, 153, 139-174.

361 Bestland, E.A., Retallack, G.J. and Swisher, C.C. (1997). Stepwise climate change recorded in
362 Eocene-Oligocene paleosol sequences from central Oregon. *The Journal of Geology*, 105, 153-
363 172.

364 Bhattacharya, J.P., and Tye, R.S. (2004). Searching for modern Ferron analogs and application
365 to subsurface interpretation. Regional to wellbore analog for fluvial-deltaic reservoir
366 modeling: The Ferron Sandstone of Utah: *AAPG Studies in Geology*, 50, 39-57.

367 Bhattacharya, J.P., Copeland, P., Lawton, T.F., and Holbrook, J. (2016). Estimation of source
368 area, river paleo-discharge, paleoslope, and sediment budgets of linked deep-time
369 depositional systems and implications for hydrocarbon potential. *Earth-Science Reviews*, 153,
370 77-110.

371 Blum, M. and Pecha, M. (2014). Mid-Cretaceous to Paleocene North American drainage
372 reorganization from detrital zircons. *Geology*, 42, 607-610.

373 Cerling, T.E. (1984). The stable isotopic composition of modern soil carbonate and its relation
374 to climate. *Earth and Planetary Science Letters*, 71, 229-240.

375 Davidson, S.K., & North, C.P. (2009). Geomorphological regional curves for prediction of
376 drainage area and screening modern analogues for rivers in the rock record. *Journal of*
377 *Sedimentary Research*, 79, 773-792.

378 Driese, S.G., Nordt, L.C., Lynn, W.C., Stiles, C.A., Mora, C.I. and Wilding, L.P. (2005).
379 Distinguishing climate in the soil record using chemical trends in a Vertisol climosequence
380 from the Texas Coast Prairie, and application to interpreting Paleozoic paleosols in the
381 Appalachian Basin, USA. *Journal of Sedimentary Research*, 75, 339-349.

382 Eide, C.H., Howell, J.A., Buckley, S.J., Martinius, A.W., Oftedal, B.T., and Henstra, G.A. (2016).
383 Facies model for a coarse-grained, tide-influenced delta: Gule Horn Formation (Early Jurassic),
384 Jameson Land, Greenland. *Sedimentology*, 63, 1474–1506.

385 Eide, C.H., Klausen, T.G., Katkov, D., Suslova, A.A. and Helland-Hansen, W. (in press). Linking
386 an Early Triassic delta to antecedent topography: source-to-sink study of the southwestern
387 Barents Sea margin. *Geological Society of America Bulletin*. doi 10.1130/B316.

388 Fedo, C.M., Sircombe, K.N., and Rainbird, R.H. (2003). Detrital zircon analysis of the
389 sedimentary record. *Reviews in Mineralogy and Geochemistry*, 53, 277–303.

390 Galloway, W.E., Whiteaker, T.L., & Ganey-Curry, P. (2011). History of Cenozoic North American
391 drainage basin evolution, sediment yield, and accumulation in the Gulf of Mexico basin.
392 *Geosphere*, 7, 938-973.

393 Gallagher, K., Brown, R., and Johnson, C. (1998). Fission track analysis and its applications to
394 geological problems. *Annual Review of Earth and Planetary Sciences*, 26, 519–572.

395 Hack, J.T. (1957). Studies of longitudinal profiles in Virginia and Maryland, U.S. Geol. Surv. Prof.
396 Pap., 294–B, 45–97.

397 Hampson, G.J., Duller, R.A., Petter, A.L., Robinson, R.A., and Allen, P.A. (2014). Mass-Balance
398 Constraints On Stratigraphic Interpretation of Linked Alluvial–Coastal–Shelfal Deposits From
399 Source To Sink: Example From Cretaceous Western Interior Basin, Utah and Colorado, USA.
400 *Journal of Sedimentary Research*, 84, 935–960.

401 Hay, W.W. (1998). Detrital sediment fluxes from continents to oceans. *Chemical geology*, 145,
402 287–323.

403 Hay, W.W. (2008). Evolving ideas about the Cretaceous climate and ocean circulation.
404 *Cretaceous Research*, 29, 725–753.

405 Hay, W.W. and Floegel, S. (2012). New thoughts about the Cretaceous climate and oceans.
406 *Earth-Science Reviews*, 115, 262–272.

407 Helland-Hansen, W., Sømme, T.O., Martinsen, O.J., Lunt, I., and Thurmond, J. (2016).
408 Dechiphering Earth's natural hourglasses: Perspectives on source-to-sink analysis. *Journal of*
409 *Sedimentary Research*, 86, 1–26.

410 Hinderer, M. (2012). From gullies to mountain belts: a review of sediment budgets at various
411 scales. *Sedimentary Geology*, 280, 21–59.

412 Holbrook, J., and Wanas, H. (2014). A fulcrum approach to assessing source-to-sink mass
413 balance using channel paleohydrologic paramaters derivable from common fluvial data sets
414 with an example from the Cretaceous of Egypt. *Journal of Sedimentary Research*, 84, 349–
415 372.

416 Kraus, M. (1999) Paleosols in clastic sedimentary rocks: their geologic applications. *Earth-*
417 *Science Reviews*, 47, 41–70.

418 Leturmy, P., Lucazeau, F., and Brigaud, F. (2003). Dynamic interactions between the Gulf of
419 Guinea passive margin and the Congo River drainage basin: 1. Morphology and mass balance.
420 *Journal of Geophysical Research: Solid Earth*, 108, 8-1–8-13.

421 Lisker, F., Ventura, B. and Glasmacher, U.A. (2009). Apatite thermochronology in modern
422 geology. In: *Thermochronological Methods: From Palaeotemperature Constraints to*
423 *Landscape Evolution Models* (Eds F. Lisker, B. Ventura and U.A. Glasmacher) Geological
424 Society, London, Special Publications, 324, 1–23.

425 Mack, G.H., and James, W.C. (1994). Paleoclimate and the global distribution of paleosols. *The*
426 *Journal of Geology*, 102, 360–366.

427 Martinsen, O.J., Sømme, T.O., Thurmond, J.B., Helland-Hansen, W., and Lunt, I. (2010). Source-
428 to-sink systems on passive margins: theory and practice with an example from the Norwegian
429 continental margin. In: *Petroleum Geology: From Mature Basins to New Frontiers –*
430 *Proceedings of the 7th Petroleum Geology Conference* (Eds B.A. Vining and S.C. Pickering)
431 Geological Society, London, Petroleum Geology Conference Series, 7, 913–920.

432 McCabe, G.J. and Wolock, D.M. (2016). Variability and Trends in Runoff Efficiency in the
433 Conterminous United States. *Journal of the American Water Resources Association*, 52, 1046–
434 1055.

435 Michael, N.A., Whittaker, A.C., and Allen, P.A. (2013). The functioning of sediment routing
436 systems using a mass balance approach: Example from the Eocene of the southern Pyrenees.
437 *The Journal of Geology*, 121, 581–606.

438 Milliman, J.D., and Farnsworth, K.L. (2011). *River discharge to the coastal ocean: a global*
439 *synthesis*, Cambridge University Press, Cambridge, UK, 349 pp.

440 Mu, Q., Heinsch, F.A., Zhao, M., and Running, S.W. (2007). Development of a global
441 evapotranspiration algorithm based on MODIS and global meteorology data. *Remote Sensing*
442 *of Environment*, 111, 519–536.

443 Müller, R., Nystuen, J.P. and Wright, V.P. (2004) Pedogenic mud aggregates and paleosol
444 development in ancient dryland river systems: criteria for interpreting alluvial mudrocks and
445 floodplain dynamics. *Journal of Sedimentary Research*, 74, 537–551.

446 Nystuen, J.P., Kjemperud, A.V., Müller, R., Adestål, V. and Schomacker, E.R. (2014). Late
447 Triassic to Early Jurassic climatic change, northern North Sea region. In: *From Depositional*
448 *Systems to Sedimentary Successions on the Norwegian Continental Margin* (Eds A.W.
449 Martinius, R. Ravnås, J.A. Howell, R.J. Steel, and J.P. Wonham), *International Association of*
450 *Sedimentologists Special Publications*, 46, 59–100.

451 Paola, C., Heller, P.L. and Angevine, C.L. (1992). The large-scale dynamics of grain-size variation
452 in alluvial basins, 1: Theory. *Basin Research*, 4, 73–90.

453 Parrish, J.T. (1998). *Interpreting pre-Quaternary climate from the geologic record*. Columbia
454 University Press, New York, 348 pp.

455 Paterson, N.W., Mangerud, G., Cetean, C.G., Mørk, A., Lord, G.S., Klausen, T.G. and Mørkved,
456 P.T. (2016). A multidisciplinary biofacies characterisation of the Late Triassic (late Carnian–
457 Rhaetian) Kapp Toscana Group on Hopen, Arctic Norway. *Palaeogeography,*
458 *Palaeoclimatology, Palaeoecology*, 464, 16–42.

459 Retallack, G.J. (1997). *Colour Guide to Paleosols*. John Wiley and Sons. Chichester, 175 pp.

460 Retallack, G.J. (2001). *Soils of the past: an introduction to paleopedology*. John Wiley and Sons.
461 Oxford, 404 pp.

462 Rigon, R., Rodriguez-Iturbe, I., Maritan, A., Giacometti, A., Tarboton, D.G., and Rinaldo, A.
463 (1996). On Hack's law. *Water Resources Research*, 32, 3367–3374.

464 Robert, C. and Kennett, J.P. (1994). Antarctic subtropical humid episode at the Paleocene-
465 Eocene boundary: Clay-mineral evidence. *Geology*, 22, 211–214.

466 Romans, B.W., Castellort, S., Covault, J.A., Fildani, A., and Walsh, J.P. (2016). Environmental
467 signal propagation in sedimentary systems across timescales. *Earth-Science Reviews*, 153, 7–
468 29.

469 Sellwood, B.W., and Valdes, P.J. (2006). Mesozoic climates: General circulation models and
470 the rock record. *Sedimentary Geology*, 190, 269–287.

471 Sun, Y., Joachimski, M.M., Wignall, P.B., Yan, C., Chen, Y., Jiang, H., Wang, L. and Lai, X. (2012).
472 Lethally hot temperatures during the Early Triassic greenhouse. *Science*, 338, 366–370.

- 473 Syvitski, J.P., and Milliman, J.D. (2007). Geology, geography, and humans battle for dominance
474 over the delivery of fluvial sediment to the coastal ocean. *The Journal of Geology*, 115, 1–19.
- 475 Sømme, T.O., Martinsen, O.J., and Lunt, I. (2013). Linking offshore stratigraphy to onshore
476 paleotopography: The Late Jurassic–Paleocene evolution of the south Norwegian margin.
477 *Geological Society of America Bulletin*, 125, 1164–1186.
- 478 Sømme, T.O., Martinsen, O.J., and Thurmond, J.B. (2009). Reconstructing morphological and
479 depositional characteristics in subsurface sedimentary systems: An example from the
480 Maastrichtian–Danian Ormen Lange system, More Basin, Norwegian Sea. *AAPG bulletin*, 93,
481 1347–1377.
- 482 Tooth, S. (2000). Process, form and change in dryland rivers: a review of recent research.
483 *Earth-Science Reviews*, 51, 67–107.
- 484 Weight, R.W., Anderson, J.B. and Fernandez, R. (2011). Rapid mud accumulation on the central
485 Texas shelf linked to climate change and sea-level rise. *Journal of Sedimentary Research*,
486 81,743–764.
- 487 Woodcock, N.H. (2004). Life span and fate of basins. *Geology*, 32, 685–688.
- 488 Wright, V.P. (1990) Equatorial aridity and climatic oscillations during the early Carboniferous,
489 southern Britain. *Journal of the Geological Society*, 147, 359-363.